Inhibition of the osteoclast V-ATPase by small interfering RNAs

Yingwei Hu, Jonas Nyman, Pirkko Muhonen, H. Kalervo Väänänen, Tiina Laitala-Leinonen*

Bone Biology Research Consortium, Department of Anatomy, Institute of Biomedicine, University of Turku, Kiinamyllynkatu 10, FIN-20520 Turku, Finland

Received 31 May 2005; revised 19 July 2005; accepted 25 July 2005

Available online 11 August 2005

Edited by Micheal R. Bubb

Abstract The multisubunit enzyme V-ATPase harbours isoforms of individual subunits. a3 is one of four 116 kDa subunit a isoforms, and it is crucial for bone resorption. We used small interfering RNA (siRNA) molecules to knock down a3 in rat osteoclast cultures. Labeled siRNA-molecules entered osteoclasts via endocytosis and knocked down the a3 mRNA. Bone resorption was decreased in siRNA-treated samples due to decreased acidification and osteoclast inactivation. Expression of a1 did not respond to decreased a3 levels, suggesting that a1 does not compensate for a3 in osteoclast cultures. Subunit a3 is thus an interesting target for novel nucleic acid therapy.
© 2005 Federation of European Biochemical Societies. Published by Elsevier B.V. All rights reserved.

Keywords: Osteoclast; V-ATPase; a3 isoform; Knockdown; siRNA

1. Introduction

Osteoclasts are large multinuclear cells specialized for resorption of mineralized bone [1]. Actively resorbing osteoclasts are highly polarized cells with four specialized membrane domains: ruffled border, sealing zone, functional secretory domain and basolateral membrane [2,3]. The low pH in the resorption lacuna is maintained by ATP-consuming vacuolar proton pumps (V-ATPase), which are present at the ruffled border membrane [4,5]. V-ATPases are essential for osteoclastic bone resorption, and V-ATPase inhibitors reduce bone resorption in vitro and in vivo [6–8].

V-ATPases are multisubunit complexes including two functional domains: a catalytic V_1 sector and membrane-spanning V_0 sector where subunit a is located. Yeast V-ATPases contain two different isoforms of subunit a that differ in their subcellular location, coupling efficiency and in vivo dissociation between V_1 and V_0 complexes [9]. In mouse and human, four subunit a isoforms have been identified [10–13]. These isoforms are differentially expressed in various tissues. Isoform a1 is found in clathrin-coated vesicles, with highest expression in brain and liver. Isoform a2 is expressed in heart, kidney, brain, and liver. Isoform a3 is highly expressed in osteoclasts and disruption of the mouse or human a3 gene results in severe osteopetrosis [14,15] including infantile malignant osteopetrosis [16–18]. Isoform a4 is expressed in kidney intercalated cells, where it is involved in the regulation of acid–base homeostasis.

The first report describing the cloning of isoform a3 indicated that this isoform was unique to the osteoclast and essential for osteoclast function [19]. Later, a3 was also detected in other tissues [10,11], but the highest expression was still found in bone [20]. In RAW267.4 cells that can be induced to form multinuclear osteoclast-like cells, a3 expression is induced during osteoclast differentiation. Subunit a3, but not a1 or a2, are located in the ruffled border membrane of actively resorbing osteoclasts [11,21]. Primary osteoclasts are hard to transfect although macrophage cell lines stimulated to differentiate into osteoclasts are transfectable with small interfering RNA (siRNA)-constructs [22–24]. The current paper describes for the first time carrier-free siRNA uptake into primary osteoclasts, where downregulation of a3 by siRNA molecules critically impairs bone resorption.

2. Materials and Methods

2.1. Design and synthesis of siRNA molecules

Three siRNA molecules targeting rat a3 coding region were designed according to Elbashir et al. [25] with Ambion's design system (www.ambion.com). The siRNA sequences shown in Table 1 were synthesized from DNA templates with the Silencer siRNA construction kit according to the suggested protocol (Ambion, USA). To analyze uptake and intracellular distribution of siRNA molecules, Cy3 labeling with Silencer siRNA labeling kit was used (Ambion, USA).

2.2. Cell culture and transfection

Cell culture reagents were obtained from Invitrogen (UK). Bone cells isolated from rat long bones were cultured on glass coverslips or bovine bone slices as described before [26]. 30 U of prime RNAse inhibitor (Eppendorf, Germany) was added to each 300 μL of culture medium 15 min before siRNA additions to inhibit RNAse activity in the medium. All siRNA molecules were used at 100 nM concentrations. Uptake of labeled siRNA-molecules into osteoclasts was monitored in samples incubated with siRNA-duplexes at +4 °C; control samples were kept at room temperature. After 45 min, cells were washed in PBS and transferred into fresh, warm culture medium. Endocytosis of membrane-bound siRNA-molecules was allowed to proceed for 0, 1, 2, 4 or 12 h prior to microscopical evaluation. The effects of siRNA-molecules on osteoclast cytoskeleton were monitored by incubating cells in the presence of siRNA-molecules for 48 h, rinsed and incubated in fresh medium for another 24 h.

2.3. RNA extraction and RT-PCR

Total RNA was extracted from siRNA-treated cells using GenElute mammalian total RNA kit (Sigma, USA) and genomic DNA was removed with DNAse (Ambion, USA). Quantitative RT-PCR was performed using the Opticon DNA Engine (MJ Research, USA) and DyNAmo SYBR Green 2-step qRT-PCR system according to the

*Corresponding author. Fax: +358 2 333 7352.
E-mail address: tilale@utu.fi (T. Laitala-Leinonen).

Abbreviations: siRNA, small interfering RNA; V-ATPase, vacuolar H-ATPase; AO, acridine orange; TRACP, tartrate-resistant acid phosphatase

0014-5793/$30.00 © 2005 Federation of European Biochemical Societies. Published by Elsevier B.V. All rights reserved.
doi:10.1016/j.febslet.2005.07.078

Table 1
siRNA molecules targeted against NM 199089

Name	Sequence (5–3)
siRNA-1 sense	CAAGUUCUAUUCAGGGACCUU
siRNA-1 antisense	GGUCCCUGAAUAGAACUUGUU
siRNA-2 sense	UGGGACAGGAAUAAAAAGCUU
siRNA-2 antisense	CUUUUUAUUCCUGUCCCAUU
siRNA-3 sense	UAAAAAGCUGGCUGGCCCAUU
siRNA-3 antisense	UGGGCCAGCCAGCUUUUUAUU
Scrambled control siRNA	
Sense	GCACCUAUGAGAGACUGACUU
Antisense	UUGCCAUUAGCUGCAGCGUUU

Scrambled control siRNA has the same nucleotide composition as siRNA-3, but lacks significant sequence homology to known genes.

Table 2
Quantitative RT-PCR primers

Target primer sequence (5′ → 3′)	Amplicon size (bp)
rat a1	
L: ACGACCTCCAAATGGTTCTG	172
R: ACTTCTGCGATCAGGCACTT	
rat a3	
L: ATGAAGGCCGTGTACCTGAC	153
R: AGCCACAGCACTCACTCCTT	
rat GAPDH	
L: CAGCAATGCATCCTGCAC	101
R: TGGCATGGACTGTGGTCA	

All primers were used at 0,5 μM concentrations and the annealing temperature was +61 °C.

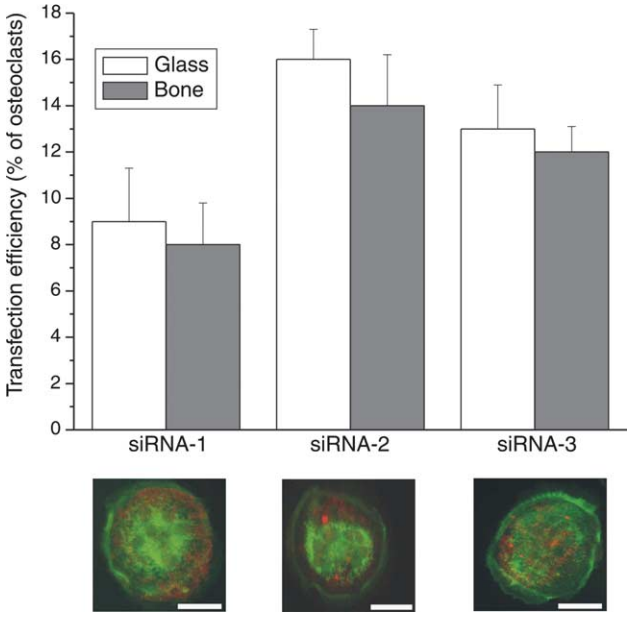

Fig. 1. Uptake of CY3-labeled siRNA molecules (red) into rat osteoclasts after 48 h. Cells were cultured on glass coverslips or bone, and actin cytoskeleton was visualized with AlexaFluor^{488}-phalloidin (green). Transfection efficiency is shown as the percentage of Cy3-positive osteoclasts of the total osteoclast number. Cy3-positive cells shown in the insets were cultured on glass. Bar = 20 μm (n = 3).

Table 3
siRNA-uptake in samples incubated at room temperature or at +4 °C to block endocytosis

	Plasma membrane staining (% of osteoclasts)	Intracellular vesicle staining (% of osteoclasts)	Cytoplasmic staining (% of osteoclasts)
RT with chase at +37 °C			
0 h	94	8	1
1 h	87	9	2
2 h	52	12	3
3 h	39	15	4
4 h	15	9	4
12 h	2	7	6
+4 °C with chase at +37 °C			
0 h	97	0	0
1 h	85	0	0
2 h	73	1	0
3 h	68	1	1
4 h	50	4	3
12 h	11	5	3

Labeled siRNA fluorescence was evaluated microscopically in 100 osteoclasts per sample group.

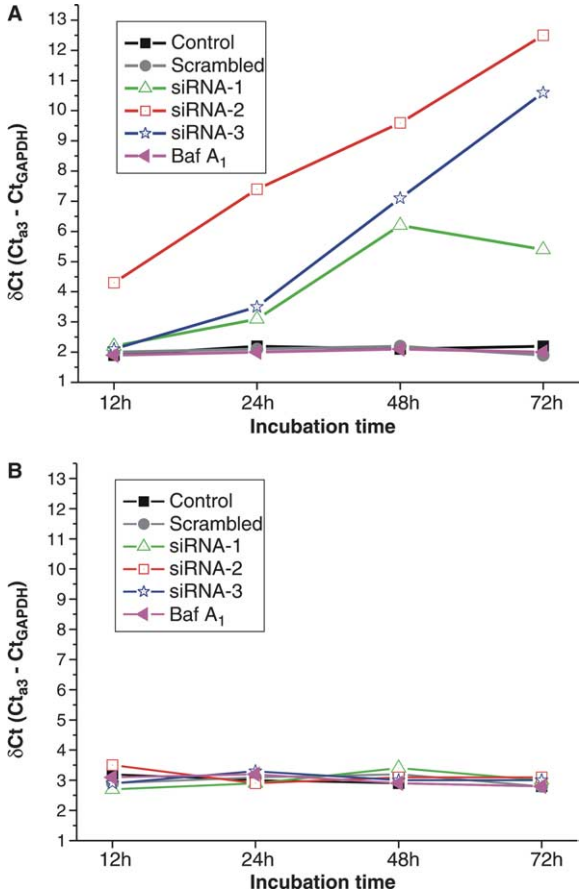

Fig. 2. Expression of subunit a isoforms a3 (A) and a1 (B) and GAPDH was monitored by quantitative RT-PCR. Total RNA was isolated from cells treated with siRNA molecules for 12 h, 24 h, 48 h or 72 h and equal amounts of total RNA was amplified with a1 or a3-specific primers using SYBR green chemistry. Cycle thresholds (C_t) were determined from the melting curves, and isoform a3 and a1 quantity was normalized with the GAPDH housekeeping gene. The ΔC_t ($C_{t\,target} - C_{t\,GAPDH}$) values are shown in the Figure, indicating that the higher the ΔC_t value, the lower the target concentration was in the original RNA sample.

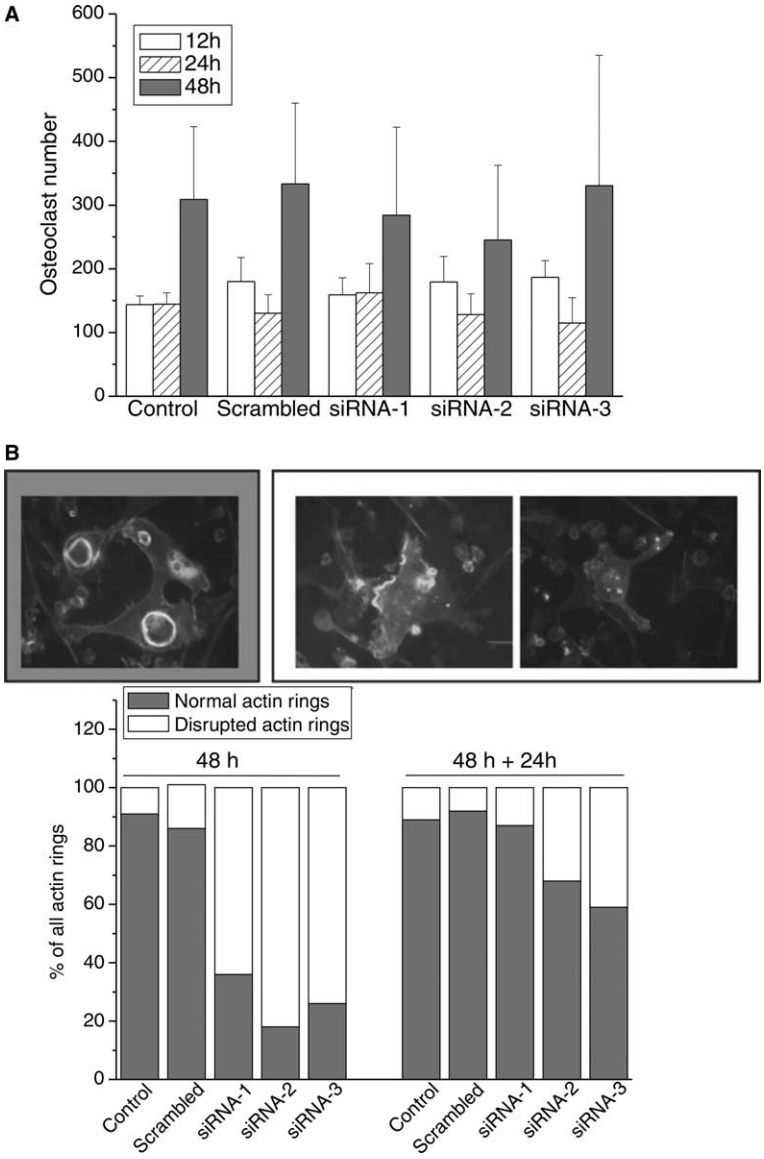

Fig. 3. (A) The number of osteoclasts was counted after TRACP-staining. TRACP-positive cells with at least three nuclei were counted as osteoclasts. Cells were incubated with siRNA duplexes for 12, 24 or 48 h prior to fixation and staining ($n = 5$). (B) The amount of normal and disrupted actin rings was counted after phalloidin staining after a 48 h siRNA-treatment (left) or from samples treated with siRNA-molecules for 48 h followed by a 24 h incubation in siRNA-free medium (right). Normal actin rings were distinguished from disrupted actin rings on morphological basis, as shown in the inset. Actin rings were counted from three bone slices for each sample group.

suggested protocol (Finnzymes, Finland). The primer sequences are shown in Table 2. Cycle tresholds (C_t) were determined and a1 and a3 fluorescence was normalized with the GAPDH reference gene fluorescence.

2.4. Stainings and microscopy

At given time points after siRNA treatment, cells were fixed with 3% paraformaldehyde–2% sucrose for 15 min. AlexaFluor^{488}-phalloidin was used to visualize actin and Hoechst was used to stain nuclei (Molecular Probes, USA). Alternatively, cells were stained for tartrate-resistant acid phosphatase (TRACP) using Leukocyte acid phosphatase kit (Sigma, USA) and osteoclasts were counted as TRACP-positive cells with at least 3 nuclei. Intracellular vesicle acidification was followed in osteoclast cultures by acridine orange (AO, Sigma, USA) uptake into live cells as described before [27]. Protein level analysis were not possible due to a lack of suitable isoform a antibodies. Samples were viewed under a Leica TCS-SP confocal microscope equipped with Argon-Crypton laser (Leica Microsystems GmbH, Germany).

2.5. Osteoclast viability and activity

To monitor cell viability, Live/Dead-system was used according to manufacturer's protocol (Molecular Probes, USA). 0.8% sodium azide-treated samples were included in the assay as a death control group. Cells were incubated with dyes for 45 min, followed by fluorescence intensity measurements using exitation/emission filter sets of 495/520 nm (for Calcein AM) and 530/642 nm (for EthD). Viability indexes were counted by dividing live cell fluorescence by dead cell fluorescence. Bone resorption was evaluated by counting WGA-lectin stained resorption pits [28] and by measuring the C-terminal cross-linked telopeptides of type I collagen (CTX) from culture medium with CrossLaps for culture kit (Nordic Biosciences, Denmark).

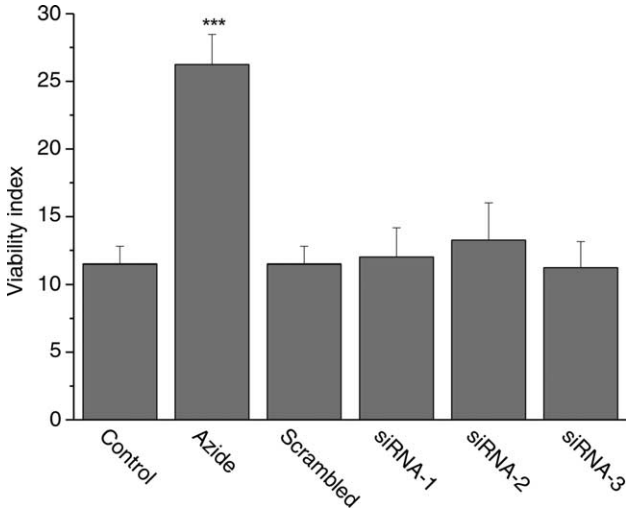

Fig. 4. Viability assay was performed on cells treated with siRNA-molecules for 48 h. Calcein AM and EthD fluorescence were measured using appropriate band pass filters. Viability index was counted by dividing Calcein AM fluorescence with EthD fluorescence. Sodium azide was included as a cell death control. ***$P < 0.001$ ($n = 4$).

Analysis of variance (ANOVA) followed by Student's t test was used for statistical analysis. Means and standard deviations (S.D.) were calculated and are shown in Figures. $P < 0.05$ was considered statistically significant.

3. Results and discussion

To confirm uptake of siRNA molecules into osteoclasts, uptake of CY3-labeled siRNA molecules was followed. Both inactive osteoclasts cultured on glass coverslips and resorbing osteoclasts cultured on bone were positive for the CY3-labeled siRNAs at all time points studied (Fig. 1). Labeled molecules were seen in distinct intracellular vesicles and diffusely in the cytoplasm. Best uptake efficiency was obtained with siRNA-2 (14 ± 2.2% of all osteoclasts) and siRNA-3 (12 ± 1.1% of all osteoclasts), while siRNA-1 was observed in only 8 ± 1.8% of all osteoclasts. Uptake and release of siRNA-molecules was also followed in cells where endocytosis was blocked by keeping the samples at +4 °C while treating the cells with siRNA-molecules (Table 3). This resulted in accumulation of labeled siRNA-molecules on the plasma membrane. When unbound siRNA-molecules were washed away and membrane-bound siRNA-molecules were allowed to be internalized by incubating the samples at +37 °C, labeled siRNA-molecules accumulated into intracellular vesicles. Labeled siRNA-molecules were time-dependently released to the cytoplasm, where a veil-like staining could be observed. At least a part of the siRNA-molecules were endocytosed by osteoclasts. Although the process was slow, the continuous low uptake seemed to be enough to account for the physiological responses seen in the cultures.

To monitor knockdown effectivity and specificity, mRNA levels were monitored with quantitative RT-PCR. Analysis of RNA samples isolated from cells treated with siRNA molecules resulted in the amplification of the expected products for rat a3 and a1 (Fig. 2). Decreased a3 mRNA levels were observed already 12 h after siRNA-2 treatment and 48 h after

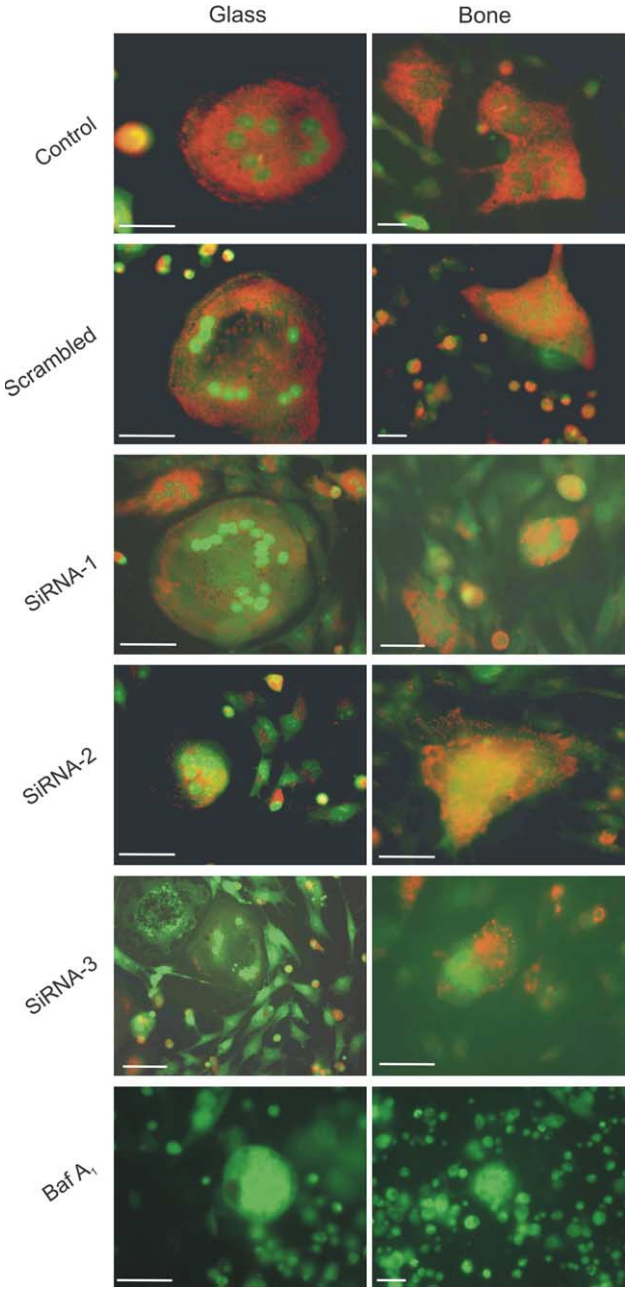

Fig. 5. Acridine orange accumulation into acidic vesicles was monitored after siRNA-treatment for 48 h. 5 nM Bafilomycin A_1 was used to inactivate V-ATPases. In neutral pH, AO is seen in green but in acidic pH the color becomes red. Cells were cultured on glass coverslips or bone. Multiple nuclei with typical green DNA-staining, and acidic vesicles with intense red staining are seen in the control osteoclasts, while no acidified compartments can be observed after Bafilomycin treatment. Bar = 20 μm, $n = 3$.

siRNA-1 and siRNA-3 treatment. The best knockdown effect was achieved with siRNA-2. No changes in a1 expression were found at the time points studied with any of our siRNA-duplexes, showing the specificity of the a3 siRNA-duplexes in knocking down isoform a3 but having no effect on a1. Isoform a3 is not exclusively osteoclast-specific and expression has been observed in a variety of tissues; mostly in liver with decreasing amounts in kidney, brain, lung, spleen, and muscle [10,11,21]. Mutations in the a3 gene cause, however, only bone pheno-

types. A possible explanation may be that other isoforms can compensate for the lack of a3 in other tissues. Yeast V-ATPases have two isoforms of subunit a: Vph1p and Stv1p. It has been shown that Stv1p can partly compensate for the lack of Vph1p when it was disrupted, leading to a less severe phenotype [29,30]. However, our data suggest that isoform a1 cannot significantly compensate for the reduced level of a3 in the osteoclast cultures.

The effects of siRNA duplexes on osteoclast number, as determined by counting TRACP-positive multinuclear cells, are shown in Fig. 3A. The number of osteoclasts remained unchanged in siRNA-treated and control cultures and no signs of induced apoptosis or decreased viability (Fig. 4) were observed. Actively resorbing osteoclasts can be distinguished by their actin ring structures [31]. As can be seen from Fig. 3B, osteoclasts treated with siRNA-molecules became inactivated and lost their actin rings, but the cells remained attached to the bone surface. When cells were first treated with siRNA-molecules for 48 h and then cultured in fresh medium for another 24 h, osteoclasts became activated and actin rings could again be seen. This is in good agreement with recent data from Karsdal et al. [32] who showed that osteoclast survival is increased when acidification is blocked. The increase in the number of inactive osteoclasts after siRNA-treatment without signs of apoptosis induction might reflect the survival effect described before.

During acidification of the resorption lacuna, V-ATPases are first transferred from intracellular vesicles to the ruffled border membrane, through which protons are then transported to the extracellular resorption site. In non-resorbing cells V-ATPases remain in the cytoplasmic vesicles which are acidic. The physiological effects of a3 knockdown were studied by monitoring changes in intravesicular acidification and in bone resorption capacity. AO is a weak base that accumulates into acidic compartments [33]. When present at high concentrations, it forms complexes resulting in a shift in fluorescence from green to red. As can be seen from Fig. 5, 5 nM Bafilomycin A_1 inhibited acidification in all cells, resulting in the neutralization of the intracellular compartments. After 48 h, all siRNA molecules inhibited AO accumulation, with the most significant inhibition obtained with siRNA-3. The observed differences in acidification knockdown in non-resorbing and resorbing osteoclasts show the importance of the physiological substrate in this type of studies.

The ultimate test for osteoclast function is their capacity to resorb bone. Upregulation of a3 expression has been detected during osteoclast differentiation and mutations in the a3 gene cause osteopetrosis in humans and in mouse [14–18]. These data show that a3 isoform plays a key role in osteoclast physiology. When the siRNA-effects on bone resorption were studied by counting the number of resorption pits (Fig. 6A) or by measuring the release of CTX-fragments into culture media (Fig. 6B), resorption was significantly decreased with 5 nM Bafilomycin A_1 and in samples treated with siRNA-2 and siRNA-3 for 48 h. Resorption pit depths remained unchanged when analyzed at 48 h (6.4 ± 2.1 μm in siRNA-1 samples, 5.9 ± 2.7 μm in siRNA-2 samples, 7.2 ± 1.9 μm in siRNA-3 samples and 6.7 ± 2.6 μm in control samples, $n = 3$).

Osteoclasts seem to endocytose small amounts of siRNA-molecules from the culture medium at individual speed. We have previously shown that antisense-molecules are spontaneously taken up into primary osteoclasts [34,35] and metacarpal

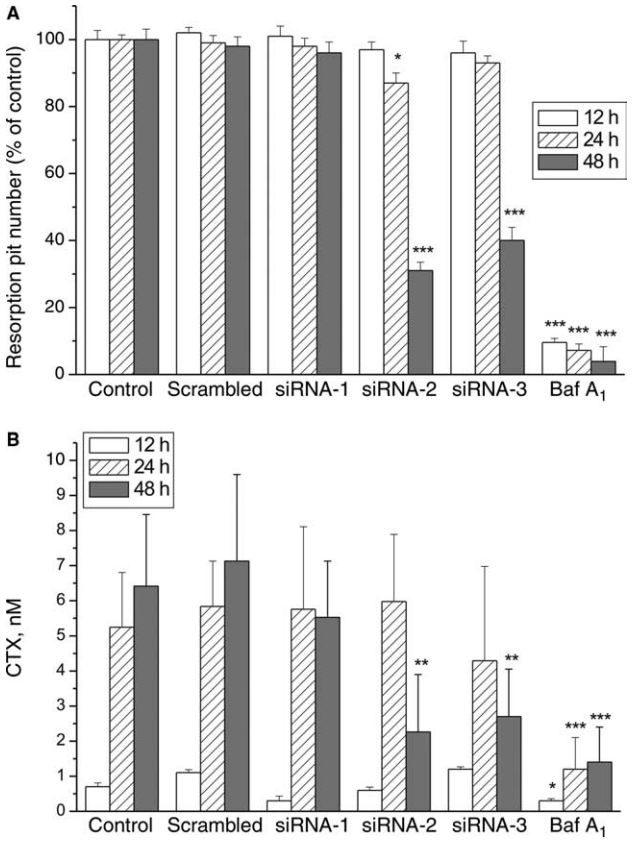

Fig. 6. Bone resorption activity in osteoclast cultures treated with siRNA-duplexes was determined after 12, 24 or 48 h. Bafilomycin A_1 was used at a 5 nM concentration to inhibit V-ATPases. (A) Resorption pits were counted after WGA-lectin staining and (B) CTX was measured from the culture media. $^*P < 0.05$; $^{**}P < 0.01$; $^{***}P < 0.001$ ($n = 4$).

tissue cultures [36]. The current data show that siRNA-treated primary osteoclasts did not die but lost their capacity to resorb bone. Despite the seemingly low transfection rate, primary osteoclasts respond to carrier-free siRNA-molecules and suggest that novel gene knockdown tools can be useful also with hard-to-transfect cells.

Acknowledgement: This work was financially supported by a EU Funded R&D Project No. QLG1-CT-2000-01801.

References

[1] Väänänen, H.K., Zhao, H., Mulari, M. and Halleen, J.M. (2000) The cell biology of osteoclast function. J. Cell Sci. 113, 377–381.
[2] Salo, J., Lehenkari, P., Mulari, M., Metsikkö, K. and Väänänen, H.K. (1997) Removal of osteoclast bone resorption products by transcytosis. Science 276, 270–273.
[3] Mulari, M.T., Zhao, H., Lakkakorpi, P.T. and Väänänen, H.K. (2003) Osteoclast ruffled border has distinct subdomains for secretion and degraded matrix uptake. Traffic 4, 113–125.
[4] Blair, H.C., Teitebaum, S.L., Ghiselli, R. and Gluck, S. (1989) Osteoclastic bone resorption by a polarized vacuolar proton pump. Science 245, 855–857.
[5] Väänänen, H.K., Karhukorpi, E.-K., Sundquist, K., Wallmark, B., Roininen, I., Hentunen, T., Tuukkanen, J. and Lakkakorpi, P. (1990) Evidence for the presence of proton pump of vacuolar H-ATPase type in the ruffled border of osteoclasts. J. Cell Biol. 111, 1305–1311.

[6] Sundquist, K., Lakkakorpi, P., Wallmark, B. and Väänänen, H.K. (1990) Inhibition of osteoclast proton transport by Bafilomycin A1 abolishes bone resorption. Biochem. Biophys. Res. Commun. 168, 309–313.
[7] Sundquist, K. and Marks Jr., S.C. (1994) Bafilomycin A1 inhibits bone resorption and tooth eruption in vivo. J. Bone Miner. Res. 9, 1575–1582.
[8] Visentin, L., Dodds, R.A., Valente, M., Misiano, P., Bradbeer, J.N., Oneta, S., Liang, X., Gowen, M. and Farina, C. (2000) A selective inhibitor of the osteoclastic V-H(+)-ATPase prevents bone loss in both thyroparathy-roidectomized and ovariectomized rats. J. Clin. Invest. 106, 309–318.
[9] Kawasaki-Nishi, S., Nishi, T. and Forgac, M. (2001) Yeast V-ATPase complexes containing different isoforms of the 100-kDa a-subunit differ in coupling efficiency and in vivo dissociation. J. Biol. Chem. 276, 17941–17948.
[10] Nishi, T. and Forgac, M. (2000) Molecular cloning and expression of three isoforms of the 100-kDa a subunit of the mouse vacuolar proton-translocating ATPase. J. Biol. Chem. 275, 6824–6830.
[11] Toyomura, T., Oka, T., Yamawuchi, C., Wada, A. and Futai, M. (2000) Three subunit a isoforms of mouse vacuolar H(+)-ATPase. Preferential expression of the a3 isoform during osteoclast differentiation. J. Biol. Chem. 275, 8760–8765.
[12] Oka, T., Murada, Y., Namba, M., Yoshimizu, T., Toyomura, T., Yamamoto, A., Sun-Wada, G.-H., Hamasaki, N., Wada, Y. and Futai, M. (2001) a4, a unique kidney-specific isoform of mouse vacuolar H^+-ATPase subunit a. J. Biol. Chem. 276, 40050–40054.
[13] Smith, A.N., Finberg, K.E., Wagner, C.A., Lifton, R.P., Devonald, M.A., Su, Y. and Karet, F.E. (2001) Molecular cloning and characterization of Atp6n1b: a novel fourth murine vacuolar H^+-ATPase a-subunit gene. J. Biol. Chem. 276, 42382–42388.
[14] Li, Y.P., Chen, W., Liang, Y., Li, E. and Stashenko, P. (1999) Atp6i-deficient mice exhibit severe osteopetrosis due to loss of osteoclast-mediated extracellular acidification. Nat. Genet. 23, 447–451.
[15] Frattini, A., Orchard, P.J., Sobacchi, C., Giliani, S., Abinun, M., Mattsson, J.P., Keeling, D.J., Andersson, A.K., Wallbrandt, P., Zecca, L., Notarangelo, L.D., Vezzoni, P. and Villa, A. (2000) Defects in TCIRG1 subunit of the vacuolar proton pump are responsible for a subset of human autosomal recessive osteopetrosis. Nat. Genet. 25, 343–346.
[16] Kornak, U., Schulz, A., Friedrich, W., Uhlhaas, S., Kremens, B., Voit, T., Hasan, C., Bode, U., Jentsch, T.J. and Kubisch, C. (2000) Mutations in the a3 subunit of the vacuolar H(+)-ATPase cause infantile malignant osteopetrosis. Hum. Mol. Genet. 9, 2059–2063.
[17] Michigami, T., Kageyama, T., Satomura, K., Shima, M., Yamaoka, K., Nakayama, M. and Ozono, K. (2002) Novel mutations in the a3 subunit of vacuolar H(+)-adenosine triphosphatase in a Japanese patient with infantile malignant osteopetrosis. Bone 30, 436–439.
[18] Scimeca, J.C., Quincey, D., Parrinello, H., Romatet, D., Grosgeorge, J., Gaudray, P., Philip, N., Fischer, A. and Carle, G.F. (2003) Novel mutations in the TCIRG1 gene encoding the a3 subunit of the vacuolar proton pump in patients affected by infantile malignant osteopetrosis. Hum. Mutat. 21, 151–157.
[19] Li, Y.P., Chen, W. and Stashenko, P. (1996) Molecular cloning and characterization of a putative novel human osteoclast-specific 116-kDa vacuolar proton pump subunit. Biochem. Biophys. Res. Commun. 218, 813–821.
[20] Manolson, M.F., Yu, H., Chen, W., Yao, Y., Li, K., Lees, R.L. and Heersche, J.N. (2003) The a3 isoform of the 100-kDa V-ATPase subunit is highly but differentially expressed in large (or =10 nuclei) and small (or = nuclei) osteoclasts. J. Biol. Chem. 278, 49271–49278.
[21] Toyomura, T., Murata, Y., Yamamota, A., Oka, T., Sun-Wada, G.-H., Wada, Y. and Futai, M. (2003) From lysosomes to the plasma membrane. Localization of vacuolar type H-ATPase with the a3 isoform during osteoclast differentiation. J. Biol. Chem. 278, 22023–22030.
[22] Hurst, I.R., Zuo, J., Jiang, J. and Holliday, L.S. (2004) Actin-related protein 2/3 complex is required for actin ring formation. J. Bone Miner. Res. 19, 499–506.
[23] TKukita, T., Wada, N., Kukita, A., Kakimoto, T., Sandra, F., Toh, K., Nagata, K., Iijima, T., Horiuchi, M., Matsusaki, H., Hieshima, K., Yoshie, O. and Nomiyama, H. (2004) RANKL-induced DC-STAMP is essential for osteoclastogenesis. J. Exp. Med. 200, 941–946.
[24] Sugatani, T. and Hruska, K.A. (2005) Akt1/Akt2 and mammalian target of rapamycin/Bim play critical roles in osteoclast differentiation and survival, respectively, whereas Akt is dispensable for cell survival in isolated osteoclast precursors. J. Biol. Chem. 280, 3583–3589.
[25] Elbashir, S.M., Harborth, J., Lendeckel, W., Yalcin, A., Weber, K. and Tuschl, T. (2001) Duplexes of 21-nucleotide RNAs mediate RNA interference in cultured mammalian cells. Nature 411, 494–498.
[26] Lakkakorpi, P., Tuukkanen, J., Hentunen, T., Järvelin, K. and Väänänen, H.K. (1989) Organization of osteoclast microfilaments during the attachment to bone surface in vitro. J. Bone Miner. Res. 4, 817–825.
[27] Palokangas, H., Mulari, M. and Väänänen, H.K. (1997) Endocytic pathway from the basal plasma membrane to the ruffled border membrane in bone-resorbing osteoclasts. J. Cell Sci. 110, 1767–1780.
[28] Selander, K., Lehenkari, P. and Väänänen, H.K. (1994) The effects of bisphosphonates on the resorption cycle of isolated osteoclasts. Calcif. Tissue Int. 55, 368–375.
[29] Manolson, M.F., Proteau, D. and Jones, E.W. (1992) Evidence for a conserved 95–120 kDa subunit associated with and essential for activity of V-ATPases. J. Exp. Biol. 172, 105–112.
[30] Manolson, M.F., Wu, B., Proteau, D., Taillon, B.E., Roberts, B.T., Hoyt, M.A. and Jones, E.W. (1994) STV1 gene encodes functional homologue of 95-kDa yeast vacuolar H(+)-ATPase subunit Vph1p. J. Biol. Chem. 269, 14064–14074.
[31] Lakkakorpi, P.T. and Väänänen, H.K. (1991) Kinetics of the osteoclast cytoskeleton during the resorption cycle in vitro. J. Bone Miner. Res. 6, 817–826.
[32] Karsdal, M.A., Henriksen, K., Sørensen, M.G., Gram, J., Schaller, S., Dziegiel, M.H., Heegaard, A.-M., Christophersen, P., Martin, T.J., Christiansen, C. and Bollerslev, J. (2005) Acidification of the osteoclastic resorption compartment provides insight into the coupling of bone formation to bone resorption. Am. J. Pathol. 166, 467–476.
[33] Palmgren, M.G. (1991) Acridine orange as a probe for measuring pH gradients across membranes: mechanism and limitations. Anal. Biochem. 192, 316–321.
[34] Laitala, T. and Väänänen, H.K. (1994) Inhibition of bone resorption in vitro by antisense RNA and DNA molecules targeted against carbonic anhydrase II or two subunits of vacuolar H^+-ATPase. J. Clin. Invest. 93, 2311–2318.
[35] Lehenkari, P., Hentunen, T., Laitala-Leinonen, T., Tuukkanen, J. and Väänänen, K. (1998) Carbonic anhydrase II plays a major role in osteoclast differentiation and bone resorption by effecting the steady state intracellular pH and Ca^{2+}. Exp. Cell Res. 242, 128–137.
[36] Laitala-Leinonen, T., Löwik, C., Papapoulos, S. and Väänänen, H.K. (1999) Inhibition of intravacuolar acidification by antisense RNA decreases osteoclast differentiation and bone resorption in vitro. J. Cell Sci. 112, 3657–3666.